


 Cite this: *Chem. Commun.*, 2023, 59, 7619

 Received 6th April 2023,  
 Accepted 25th May 2023

DOI: 10.1039/d3cc01673k

rsc.li/chemcomm

**The conjugation of photoactive benzophenone with diphenylalanine yielded a self-assembling photocatalyst that was probed in the E → Z photoisomerisation of stilbene derivatives.**

Since its discovery in 2003,<sup>1</sup> the self-assembling ability of diphenylalanine (Phe-Phe) as a minimalistic motif has inspired scientists worldwide to design dynamic functional structures for various uses.<sup>2,3</sup> In particular, supramolecular catalysis exploiting peptide derivatives has been gaining momentum, with several reported examples mimicking enzymes.<sup>4–7</sup> Recently, photocatalytic hydrogen production was attained using self-assembling porphyrin-dipeptides.<sup>8</sup> However, the combination of photoactive organic molecules with peptide assembly to catalyse organic transformations has been seldom explored. Ulijn, Braunschweig and co-workers described self-assembling conjugates of the chromophore diketopyrrolopyrrole with amino acids (Phe, Tyr, Leu) that produced <sup>1</sup>O<sub>2</sub> under light illumination for the photo-oxidation of organic sulfides into sulfoxides, with high yields and without over-oxidation.<sup>9</sup> Given the wide interest in photocatalysis applied to organic transformations, especially as a green tool for fine chemicals synthesis,<sup>10,11</sup> this area certainly deserves further investigation.

# Self-assembly of benzophenone-diphenylalanine conjugate into a nanostructured photocatalyst†

 Simone Adorinni,<sup>id</sup> <sup>a</sup> Giulio Goti,<sup>id</sup> <sup>b</sup> Lorenzo Rizzo,<sup>id</sup> <sup>b</sup> Federica Grassi,<sup>b</sup> Slavko Kralj,<sup>id</sup> <sup>cd</sup> Fatima Matroodi,<sup>e</sup> Mirco Natali,<sup>id</sup> <sup>f</sup> Rita De Zorzi,<sup>id</sup> <sup>a</sup> Silvia Marchesan<sup>id</sup> <sup>\*a</sup> and Luca Dell'Amico<sup>id</sup> <sup>\*b</sup>

In this work, we conjugated self-assembling Phe-Phe with benzophenone (BP) into *N*-(3-benzoylbenzoyl)-Phe-Phe **1** (BP-Phe-Phe, Scheme 1). The choice for BP as chromophore is motivated by its high stability, low cost, rapid intersystem crossing ( $k_{ISC} \sim 10^{11} \text{ s}^{-1}$ ), and high efficiency ( $\Phi_{ISC} = 1$ ).<sup>12</sup> Further, its aromatic nature and H-bond accepting ability may be advantageous to engage in non-covalent interactions with the substrate, and to take part in the supramolecular structuring promoted by Phe-Phe. In addition, BP is well-known as triplet sensitiser profiling the possible use of BP-Phe-Phe **1** under unconventional supramolecular photocatalysed processes.<sup>13</sup>

We began our study with the synthesis of BP-Phe-Phe **1**, which was prepared by solid-phase peptide synthesis, treating a BP carboxylic acid derivative just like an amino acid. Molecular identity and purity were confirmed by spectroscopic data (1D <sup>1</sup>H- and <sup>13</sup>C-NMR, ESI-MS, see ESI†).

Single-crystal X-ray diffraction (XRD, Fig. 1) revealed the ability of BP-Phe-Phe to yield amphiphilic stacks held together mainly by H-bonds through the peptide backbone (2.9 Å) and between the C-termini (2.7 Å). Despite the hydrophobic character of **1**,  $\pi$ - $\pi$  interactions are weak, with quite long centre-to-centre distance (5 Å) and significant offset (4 Å). The C<sub>BP</sub>-N<sub>1</sub>-C<sub>α1</sub>-C<sub>1</sub> torsion angle (Fig. S12, ESI†) can be compared to the  $\phi$  dihedral angle of proteins, while the angle N<sub>1</sub>-C<sub>α1</sub>-C<sub>1</sub>-N<sub>2</sub> corresponds to the  $\psi$  dihedral angle. The values measured in the crystal structure for these two torsion angles (−112.6° and 121.4°, respectively) suggest a backbone conformation similar

<sup>a</sup> Chemical and Pharmaceutical Sciences Dept., University of Trieste, V. Giorgieri 1, Trieste 34127, Italy. E-mail: smarchesan@units.it

<sup>b</sup> Chemical Sciences Dept., University of Padova, V. Marzolo 1, Padova 35131, Italy. E-mail: luca.dellamico@unipd.it

<sup>c</sup> Materials Synthesis Dept., Jožef Stefan Institute, Jamova 39, Ljubljana 1000, Slovenia

<sup>d</sup> Pharmaceutical Technology Dept., University of Ljubljana, Aškerčeva 7, Ljubljana 1000, Slovenia

<sup>e</sup> Elettra Sincrotrone Trieste, Basovizza, Trieste 34149, Italy

<sup>f</sup> Department of Chemical, Pharmaceutical, and Agricultural Sciences, University of Ferrara, V. Borsari 46, Ferrara 44121, Italy

 † Electronic supplementary information (ESI) available: Materials and methods, <sup>1</sup>H- and <sup>13</sup>C-NMR spectra, ESI-MS spectra, self-assembly tests, TEM data, XRD analysis, CD data, microRaman spectra, UV-Vis and emission spectra, photoisomerization kinetics study and products' <sup>1</sup>H-NMR data. CCDC 2250023. For ESI and crystallographic data in CIF or other electronic format see DOI: <https://doi.org/10.1039/d3cc01673k>


**Scheme 1** Self-assembling photocatalyst with benzophenone (BP) and Phe-Phe.



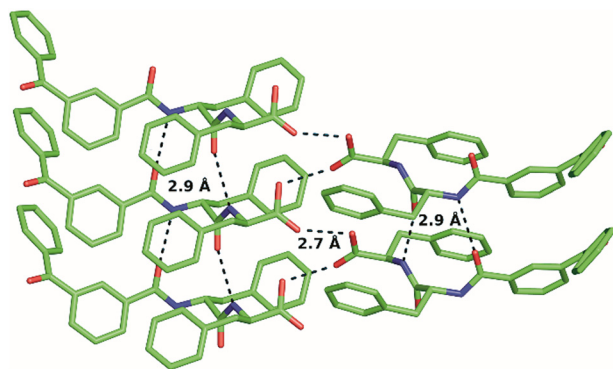


Fig. 1 Single-crystal XRD structure of BP-Phe-Phe stacks held together by H-bonds (dashed lines) between amide groups and between C-termini (CCDC 2250023).

to that of  $\beta$ -sheets.<sup>14</sup> The amyloid nature was confirmed by a fluorescence assay with Thioflavin T, which binds to fibrils composed of  $\beta$ -stacks.<sup>15,16</sup> The derived critical aggregation concentration (cac)<sup>17</sup> corresponded to 1.0 mM (Fig. 2A), and fibrils were confirmed by transmission electron microscopy (TEM, Fig. 2B), with an average diameter of  $23.4 \pm 11.4$  nm ( $n = 150$  counts, Fig. 2C).

FT-IR of the amide region confirmed H-bound COOH groups ( $1719\text{ cm}^{-1}$ ), and amide signals typical of  $\beta$ -stacks ( $1627$ ,  $1538$ ,  $1453$ ,  $1242\text{ cm}^{-1}$ ) (Fig. 2D). Circular dichroism (CD) spectra displayed a minimum at  $240$  nm (see ESI†) that was attenuated by light scattering from fibrillation, which reached a plateau within  $30$  min. (Fig. 2E). Phe aromatic signals usually occur at  $220$ – $230$  nm, with redshifts being reported as a result of self-assembly,<sup>18</sup> while  $^1L_a$  transitions of benzamides resulted in strong signals also at the higher  $\lambda$  of  $230$ – $250$  nm.<sup>19</sup>

Visible-light Raman spectra of the fibrils matched those of the crystals (see ESI†), from which we inferred analogous packing. Having assessed the ability of BP-Phe-Phe to generate fibrils, we next evaluated the possibility of using these supramolecular assemblies to catalyse photoisomerization processes.<sup>20</sup> In particular, we targeted the photoisomerization of *E*-stilbenes (*E*-2, Fig. 3A),<sup>21–23</sup> comparing the activity of BP-Phe-Phe **1** with the model compound BP methyl ester (BP-OMe) **4** lacking Phe-Phe (*vide infra*). Firstly, the photophysical properties of **1** were investigated (at a concentration  $\geq$  cac, Fig. 3B–D).

The UV-Vis spectrum of BP-Phe-Phe **1** (in MeCN, Fig. 3B) displayed a strong absorption at  $252$  nm, assigned to  $\pi \rightarrow \pi^*$  transition,<sup>24</sup> with an attenuation coefficient  $\epsilon = 20\,916\text{ M}^{-1}\text{ cm}^{-1}$  that was slightly higher than BP alone ( $\epsilon = 19\,400\text{ M}^{-1}\text{ cm}^{-1}$ ), due to a favourable effect of Phe-Phe that increased its ability to absorb light. The shoulder with a maximum at  $340$  nm ( $\epsilon = 138\text{ M}^{-1}\text{ cm}^{-1}$ ), due to a  $n \rightarrow \pi^*$  symmetry-forbidden transition, gave scope for photocatalysis with a light-emitting diode (LED) at  $390$  nm (*vide infra*). The triplet state ( $T_1$ ) of BP-Phe-Phe has an energy of  $E_{00} = 3.00\text{ eV}$  ( $69\text{ kcal mol}^{-1}$ ), as determined by luminescence measurements at  $77\text{ K}$ , and a lifetime of  $55\text{ }\mu\text{s}$  in MeCN, as measured by laser flash photolysis (Fig. 3D). The model compound BP-OMe **4**, on the other hand, showed a similar energy, but a slightly shorter lifetime of  $44\text{ }\mu\text{s}$  (see ESI†).

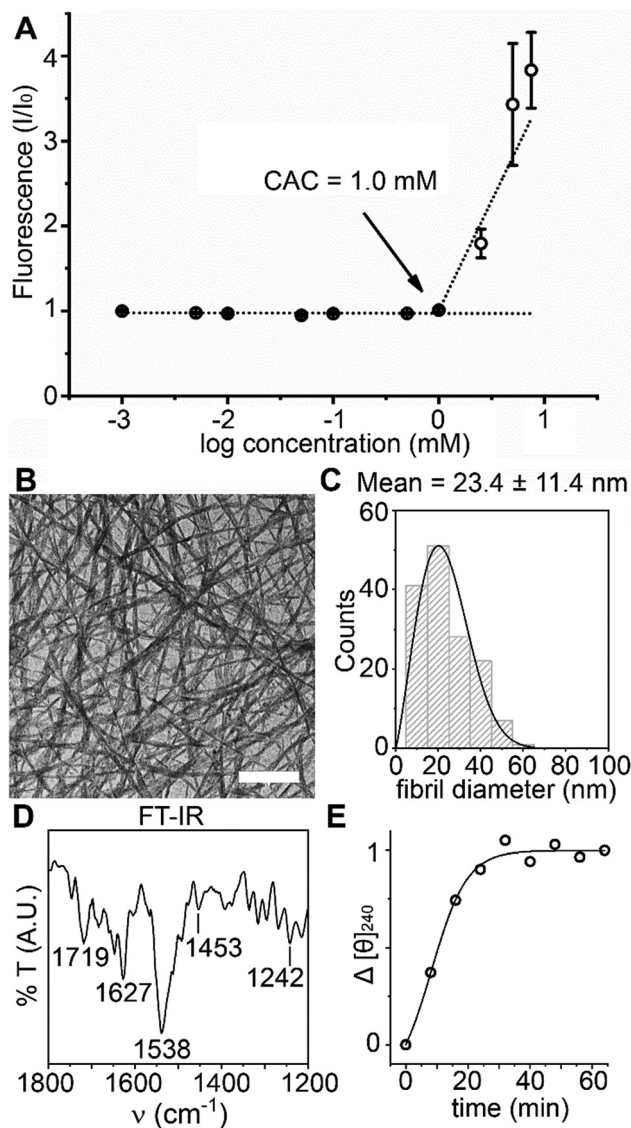


Fig. 2 Fibrillation of BP-Phe-Phe. (A) Critical aggregation concentration (cac) derived from the Thioflavin-T fluorescence assay. (B) TEM micrograph. Scalebar =  $500$  nm. (C) Fibril diameter distribution from TEM micrographs. (D) FT-IR spectra of the amide region. (E) Fibrillation kinetics monitored by CD evolution of the minimum at  $240$  nm.

Interestingly, the supramolecular assembly neither quenched nor interfered with the excited state of the chromophore unit, profiling its potential use in catalysis.

Next, we probed the possibility of the catalyst to interact with the substrate. UV-Vis spectra of *E*-stilbene **2** ( $0.5$ – $2.0$  mM) without or with BP-Phe-Phe ( $1.0$  mM, cac) revealed an evident hypochromic effect and a minor bathochromic shift (Fig. 3E), compatible with the formation of *J*-aggregates, that was absent in the case of BP-OMe **4** (Fig. S17, ESI†). Both effects were confirmed by the spectral modifications of the Raman signals associated to the aromatic vibrations, observed in the UV Resonance Raman (UVR) spectra collected in solution with  $\lambda_{\text{ex}} = 266$  nm (Fig. 3F). In particular, the bathochromic shift of the BP-Phe-Phe aromatic signal centred at  $1600\text{ cm}^{-1}$  was more





**Fig. 3** (A) Photoisomerisation of *E*-stilbene (*E*-2). (B) UV-Vis spectra of BP-Phe-Phe. (C) BP-Phe-Phe emission spectrum (ex. 315 nm). (D) BP-Phe-Phe triplet state lifetime. (E) UV-Vis spectra of stilbene without and with BP-Phe-Phe (1 mM, cac). (F) UVRR spectra of BP-Phe-Phe, stilbene, and their mixtures, all in MeCN.

pronounced in the presence of an equimolar mixture of *E*- and *Z*-stilbene ( $4 \text{ cm}^{-1}$ ) than *E*-stilbene ( $2 \text{ cm}^{-1}$ ), suggesting supramolecular interactions between both isomers and the catalyst. *J*-aggregates are well-known to stabilise excitons of the participating species through delocalisation,<sup>25</sup> and could have a favourable effect in the photocatalytic *E*-*Z* isomerisation in the presence of BP-Phe-Phe **1**. With these promising findings in hand, we investigated the catalytic activity of **1** as photosensitiser under 390 nm LED irradiation. We initially realised that the catalyst loading was a key parameter for the reaction. Indeed, when using  $>1 \text{ mol}\%$  catalyst loading, the formation of large fibres was visible to the naked eye (see ESI†). These supramolecular structures could negatively impact on the reaction outcome by scattering phenomena. In fact, we observed the best results when using a catalyst loading as low as  $1 \text{ mol}\%$  (Table 1 entry 3 vs. entries 1, 2). At this concentration the fibrils have a diameter of 23 nm and a more homogeneous

**Table 1** *E*-stilbene **2** photoisomerisation optimization<sup>a</sup>

| Entry          | PC (mol%)           | Light   |             | Time (h) | Yield <sup>b</sup> (%) | <i>Z</i> : <i>E</i> <sup>b</sup> |
|----------------|---------------------|---------|-------------|----------|------------------------|----------------------------------|
|                |                     | Fibrils | source (nm) |          |                        |                                  |
| 1              | <b>1</b> (5 mol%)   | Yes     | 390         | 5        | 92                     | 38:62                            |
| 2              | <b>1</b> (2.5 mol%) | Yes     | 390         | 5        | 87                     | 46:54                            |
| 3              | <b>1</b> (1 mol%)   | Yes     | 390         | 5        | 90                     | 43:57                            |
| 4              | <b>1</b> (1 mol%)   | Yes     | 390         | 7        | 94                     | 62:38                            |
| 5              | <b>1</b> (1 mol%)   | Yes     | 405         | 5        | 81                     | 7:93                             |
| 6 <sup>c</sup> | <b>1</b> (1 mol%)   | No      | 390         | 7        | 89                     | 39:61                            |
| 7              | <b>3</b> (1 mol%)   | No      | 390         | 7        | 73                     | 38:72                            |
| 8              | <b>4</b> (1 mol%)   | No      | 390         | 7        | 94                     | 51:43                            |
| 9              | —                   | —       | 390         | 7        | <5                     | —                                |

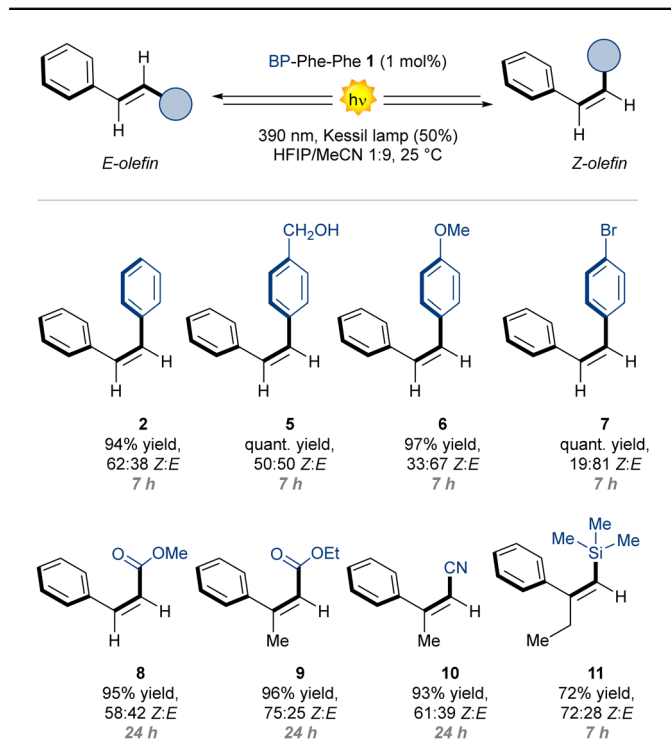
<sup>a</sup> Unless otherwise noted, reaction conditions: stilbene *E*-2 (0.1 mmol), photocatalyst (1 μmol, 1.0 mM), HFIP (0.1 mL), MeCN (0.9 mL), 50 rpm.  
<sup>b</sup> The yields and the *Z*:*E* ratios were calculated by <sup>1</sup>H-NMR using 1,3,5-trimethoxybenzene as internal standard and CG-FID. <sup>c</sup> Reaction run at 1000 rpm.

distribution (Fig. 2C), resulting in high surface area, and giving the best result after 7 h of reaction (entry 4, 94% yield, 62:38 *Z*:*E*). When trying to perform the reaction using more red-shifted wavelengths, a significant drop in yield for the *Z* isomer was observed (entry 5), in agreement with the UV-Vis spectrum of BP-Phe-Phe **1** (Fig. 3B).

We next performed a series of control experiments evaluating the impact of both the supramolecular aggregates, as well as the Phe-Phe unit on the photoisomerisation reaction. When fibrillation was hampered by vigorous stirring at 1000 rpm, the yield of *Z* stilbene dropped (entry 6, 89% yield, 39:61 *Z*:*E*), indicating that fibrils resulted in improved catalytic performances. This finding was also in agreement with the UVRR analysis that suggested an interaction between the substrate and the fibrils. We next compared the results with other homogeneous sensitizers (entry 7 and 8). Benzophenone **3**, furnished stilbene **2** in 73% yield and 38:72 *Z*:*E* selectivity (entry 7), while the carboxymethyl BP methyl ester **4** gave very similar results relative to the homogeneous system (entry 8 vs. 6). To rationalise the improved performances in the presence of the supramolecular fibrils (entry 4 vs. 8), we performed two kinetic experiments (up to 12 h), with PC **1** and **4** (see ESI†). Both systems reached a photostationary state equilibrium after 7 h. We inferred that, for the supramolecular assembly, such equilibrium is set to a higher value of *Z*:*E* ratio relative to the homogeneous system. Without PC, no reaction was observed, excluding a direct excitation pathway (entry 9). With the optimised conditions in hand, we evaluated the generality of the developed photocatalysed process for a series of diverse olefins (Table 2). Interestingly, stilbene derivatives with electron-



**Table 2** Survey of *E*-olefins **2–11** that undergo photoisomerization catalysed by BP-PhePhe **1**. Reaction conditions: stilbene *E-2* (0.1 mmol), BP-PhePhe **1** (1 μmol, 1.0 mM), HFIP (0.1 mL), MeCN (0.9 mL). The yields and the *Z*:*E* ratios were calculated by <sup>1</sup>H-NMR using 1,3,5-trimethoxybenzene as internal standard



donating or electron-withdrawing groups (*E*-**5–7**) proved to be competent substrates, with *Z*/*E* selectivities ranging from 19:81 (**7**) to 50:50 (**5**). We next evaluated  $\alpha,\beta$ -unsaturated esters and nitriles (*E*-**8–10**).<sup>26,27</sup> In these cases, with a longer reaction time of 24 h, we observed high yields and good selectivities, up to 75:25 (**9**). The trisubstituted *E*-trimethylsilyl styrene **11** also delivered the isomerization product in 72% yield and 72:28 *Z*:*E* ratio.<sup>28</sup>

In summary, we reported the preparation, characterisation, and application of BP-Phe-Phe **1** as a general and efficient minimalistic nanofibrillator exerting synthetically useful photocatalytic activity in its supramolecular state. Photoactive fibrils of **1** efficiently catalysed the photoisomerisation of diverse olefins (yields up to 75%) with a catalyst-loading as low as 1 mol%. Interestingly, the homogeneous conditions resulted in inferior performances, indicating the key role of the supramolecular fibril in interacting with the olefins to promote photoisomerisation, as confirmed by spectroscopic and vibrational studies, also using advanced techniques with synchrotron irradiation. These results highlight the feasibility of using self-assembled photocatalysts for organic synthesis.

This work was supported by MUR PRIN 2020927WY3 “Electrolight4Value” (L. D. and M. N.), ERC-StG 2021 SYNPHOCAT 101040025 (L. D.), SRA-ARRS grant P2-0089, and ARRS grants J2-3043, J3-3079, J7-4420 (S. K.). G. G. thanks MUR for a Young Researchers, Seal of Excellence fellowship. We acknowledge Elettra Sincrotrone Trieste for access to synchrotron XRD1 and

IUVS beamlines. F. M. thanks funding by TRIL Program of the Abdus Salam International Centre for Theoretical Physics (ICTP). A. S. thanks the RSC Surface Reactivity and Catalysis Group (SURCAT) for support. The authors thank the CEMM Nanocenter (JSI, Slovenia) for TEM access.

## Conflicts of interest

There are no conflicts to declare.

## Notes and references

‡ For the correct preservation of the fibrils, the reaction must be conducted at  $25 \pm 2$  °C, not exceeding gentle stirring of 50 rpm.

- M. Reches and E. Gazit, *Science*, 2003, **300**, 625–627.
- M. Amit, S. Yuran, E. Gazit, M. Reches and N. Ashkenasy, *Adv. Mater.*, 2018, **30**, e1707083.
- F. Sheehan, D. Sementa, A. Jain, M. Kumar, M. Tayarani-Najjaran, D. Kroiss and R. V. Uljijn, *Chem. Rev.*, 2021, **121**, 13869–13914.
- C. Rizzo, S. Marullo, F. Billeci and F. D’Anna, *Eur. J. Org. Chem.*, 2021, 3148–3169.
- I. W. Hamley, *Biomacromolecules*, 2021, **22**, 1835–1855.
- Y. Lou, B. Zhang, X. Ye and Z.-G. Wang, *Mater. Today Nano*, 2023, **21**, 100302.
- O. Zozulia, M. A. Dolan and I. V. Korendovych, *Chem. Soc. Rev.*, 2018, **47**, 3621–3639.
- E. Nikoloudakis, M. Pigiaki, M. N. Polychronaki, A. Margaritopoulou, G. Charalambidis, E. Serpetzoglou, A. Mitraki, P. A. Loukakos and A. G. Coutsolelos, *ACS Sustainable Chem. Eng.*, 2021, **9**, 7781–7791.
- S. Biswas, M. Kumar, A. M. Levine, I. Jimenez, R. V. Uljijn and A. B. Braunschweig, *Chem. Sci.*, 2020, **11**, 4239–4245.
- G. E. M. Crisenza and P. Melchiorre, *Nat. Commun.*, 2020, **11**, 803.
- M. Oelgemöller, *Chem. Rev.*, 2016, **116**, 9664–9682.
- N. A. Romero and D. A. Nicewicz, *Chem. Rev.*, 2016, **116**, 10075–10166.
- J. Mateos, S. Cuadros, A. Vega-Peñaloza and L. Dell’Amico, *Synlett*, 2021, 116–128.
- G. N. Ramachandran, C. Ramakrishnan and V. Sasisekharan, *J. Mol. Biol.*, 1963, **7**, 95–99.
- N. Amdursky, Y. Erez and D. Huppert, *Acc. Chem. Res.*, 2012, **45**, 1548–1557.
- M. Biancalana and S. Koide, *Biochim. Biophys. Acta, Proteins Proteomics*, 2010, **1804**, 1405–1412.
- V. Castelletto, P. Ryumin, R. Cramer, I. W. Hamley, M. Taylor, D. Allsop, M. Reza, J. Ruokolainen, T. Arnold, D. Hermida-Merino, C. I. Garcia, M. C. Leal and E. Castaño, *Sci. Rep.*, 2017, **7**, 43637.
- N. Amdursky and M. M. Stevens, *Chem. Phys. Chem.*, 2015, **16**, 2768–2774.
- B. Ringdahl, *Acta Chem. Scand., Ser. B*, 1984, **B38**, 141.
- T. Nevesely, M. Wienhold, J. J. Molloy and R. Gilmour, *Chem. Rev.*, 2022, **122**, 2650–2694.
- J. Saltiel, J. E. Mace, L. P. Watkins, D. A. Gormin, R. J. Clark and O. Dmitrenko, *J. Am. Chem. Soc.*, 2003, **125**, 16158–16159.
- D. C. Fabry, M. A. Ronge and M. Rueping, *Chem. – Eur. J.*, 2015, **21**, 5350–5354.
- W. Cai, H. Fan, D. Ding, Y. Zhang and W. Wang, *Chem. Commun.*, 2017, **53**, 12918–12921.
- N. J. Turro, V. Ramamurthy and J. C. Scaiano, *Modern Molecular Photochemistry of Organic Molecules*, University Science Books, Sausalito, California (USA), 2010.
- N. J. Hestand and F. C. Spano, *Chem. Rev.*, 2018, **118**, 7069–7163.
- J. B. Metternich and R. Gilmour, *J. Am. Chem. Soc.*, 2015, **137**, 11254–11257.
- J. B. Metternich, S. Sagebiel, A. Lückener, S. Lamping, B. J. Ravoo and R. Gilmour, *Chem. – Eur. J.*, 2018, **24**, 4228–4233.
- S. I. Faßbender, J. J. Molloy, C. Mück-Lichtenfeld and R. Gilmour, *Angew. Chem., Int. Ed.*, 2019, **58**, 18619–18626.

